ARTICLES

Transient response of a capsule subjected to varying flow conditions: Effect of internal fluid viscosity and membrane elasticity

A. Diaz
UMR CNRS 6600, UTC, Compiègne, France

N. Pelekasis
Laboratory of Computational Fluid Dynamics, Chemical Engineering, University of Patras, Greece

D. Barthès-Biesel[a)]
UMR CNRS 6600, UTC, Compiègne, France

(Received 23 July 1999; accepted 13 January 2000)

The *transient* deformation of an axisymmetric capsule freely suspended in a pure straining flow is studied, for sudden or periodic variations of the intensity of the rate of strain. The particle Reynolds number is supposed to be very small and the problem is solved numerically by means of the boundary integral method. In the case of a sudden start of flow, the time response of the capsule can be approximated by an exponential function, and is thus characterized by only two parameters: the equilibrium deformation D_∞ and the characteristic response time τ_s. The respective influence of viscosity ratio, membrane elasticity, and initial particle geometry is analyzed. The dynamic response of the capsule subjected to periodic variations of the rate of strain is also studied. The response time τ_s appears to be an appropriate parameter to estimate the capsule adaptability to changing flow conditions. © *2000 American Institute of Physics.* [S1070-6631(00)00605-X]

I. INTRODUCTION

A capsule consists of an internal medium (pure or complex liquid), enclosed by a deformable membrane. Capsules are frequently met in nature (blood cells) or in industrial processes (pharmaceutical, cosmetic, or food industry). In natural as well as in industrial situations, capsules are often suspended in a flowing liquid. In response to hydrodynamic forces, the particles deform and sometimes even break up. One must be able to predict the behavior of a capsule in flow, in order to evaluate its suitability for a given application or to prevent breakup. The analysis of the motion and deformation of a capsule involves the solution of two fluid mechanics problems (flow in the internal and in the external liquids) coupled with a solid mechanics problem (deformation of the interfacial membrane). The suspending fluid and the particle internal liquid are usually supposed to be incompressible and Newtonian. Owing to the small dimensions of the capsule, the particle Reynolds number is very small, so that the Stokes equations can be used. Even with this simplification, the problem is nonlinear because it is of the free surface type and also because the deformation of the membrane may be large. Furthermore, several intrinsic physical properties of the capsule govern the process, such as geometry at rest, membrane constitutive properties, and internal viscosity. The respective influence of these parameters has yet to be fully understood.

Over the years many studies have been devoted to capsule mechanics. Analytical solutions based on a perturbation expansion of the equations are available for initially spherical capsules subjected to small deformations.[1] Such solutions have a limited range of validity and cannot deal with nonspherical capsules (e.g., red blood cells) undergoing large deformations. In order to overcome those shortcomings, current research in the field has resorted to numerical models. Such approaches are based on an integral formulation of the Stokes equations, which is particularly well adapted to free surface problems. For computational reasons, almost all models have dealt with flow situations where the ratio λ between the internal and external fluid viscosity is unity. This restriction is not important if one is interested only in steady-state results and if the flow geometry is such that all internal motion has stopped at equilibrium. This is the case in axisymmetric situations where an axisymmetric capsule is suspended in a pure straining motion[2,3] or moves along the axis of a cylindrical channel.[4] The effect of membrane rheology and initial geometry on the steady deformation of a capsule can then be assessed. In particular, it is possible to predict the burst of the capsule when the shear strength exceeds a critical value. Three-dimensional (3D) flow situations have also been considered[5,6] where the capsule is suspended in a simple shear flow with $\lambda = 1$. The effect of the

[a)]Author to whom correspondence should be addressed; electronic mail: dbb@utc.fr

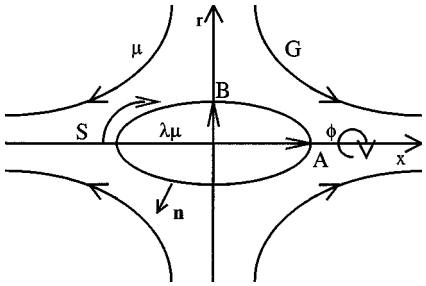

FIG. 1. Axisymmetric capsule suspended in pure axial straining flow.

viscosity ratio λ on the motion of a capsule in a simple shear flow has been also investigated.[7]

All the aforementioned studies are mostly focused on the determination of a *steady* situation, although the numerical algorithms usually follow the transient behavior of a capsule after a sudden start of the flow. So there is only scant information on the response time of a capsule. In particular, the effect of the particle physical properties has not been studied in detail. In practical problems, however, a capsule may be subjected to a time varying flow (startup of flow, oscillatory flow). Furthermore, a steady flow may appear unsteady in a reference frame linked to the particle. This is the case when the capsule flows in a channel with a variable cross section (microcirculation, filtration, flow in a porous medium). In order to estimate the adaptation of the capsule shape to the local flow conditions, it is useful to know the particle intrinsic response time and compare it to the residence time.

It is the objective of the present paper to study the transient response of a capsule to a time-dependent external flow field. The respective influence of internal viscosity, membrane mechanical properties, and initial particle geometry (specifically the surface-to-volume ratio) is considered. A pure straining flow situation is chosen for various reasons. First, it is already well documented for the case $\lambda=1$.[2,3] Second, owing to the symmetry of the problem, the final steady state does not depend on λ. This provides a useful check on the numerical precision of the results. Third, since the problem is axisymmetric, its dimension is reduced by one, thus keeping the computational time within reasonable limits. It should also be noted that this flow situation is an approximation to the entrance problem of a small capsule convected toward a pore. Finally, the quantitative information obtained for this flow may serve as an estimate for other types of linear flows.

The governing equations of the problem are presented in Sec. II, the numerical procedure is outlined in Sec. III, whereas Sec. IV is devoted to the presentation and the discussion of the numerical results.

II. PROBLEM STATEMENT

We consider a capsule that consists of a drop of a Newtonian incompressible liquid of viscosity $\lambda\mu$, enclosed by an infinitely thin membrane (M). The membrane is characterized by a surface elastic modulus E_s and has negligible bending resistance. The particle reference geometry is a spheroid with diameter $2A$ and radius B (Fig. 1). The capsule is freely suspended in an unbounded Newtonian incompressible fluid with viscosity μ. Far from the particle, the external flow is axisymmetric and corresponds to an axial straining motion of intensity G,

$$v_x^\infty = Gx, \quad v_r^\infty = -\tfrac{1}{2}Gr, \quad v_\phi^\infty = 0, \tag{2.1}$$

in dimensional variables. The particle axis is aligned with the flow axis, and the problem is axisymmetric. Cylindrical coordinates (r, ϕ, x) are used. Nondimensional variables are used throughout: lengths are scaled with $L=(AB^2)^{1/3}$, time with a characteristic scale t_0 to be defined later, velocities by L/t_0, viscous stresses by μ/t_0, and elastic tensions by E_s. Since the capsule has both elasticity and viscosity, it is possible to define an intrinsic time scale for the particle,

$$t_c = \lambda\mu L/E_s.$$

The capillary number ε is the ratio of external viscous forces to elastic forces and is thus defined by

$$\varepsilon = \mu G L/E_s.$$

A. Capsule deformation

In the reference configuration, the membrane points on a meridian curve are labeled by their cylindrical coordinates (X, R) and by the arc length S ($S=0$ where $R=0$ and $X=-A$). In the deformed configuration, the membrane points coordinates are $[x(S,t),r(S,t)]$, with arc length $s(S,t)$ ($s(0,t)=0$). The principal directions of stress and strain are along the meridian (index s) and azimuth (index ϕ) so that the equations describing the mechanics of the membrane simplify significantly. Indeed, the membrane deformation may be defined in terms of the principal extension ratios λ_s and λ_ϕ,

$$\lambda_s = \frac{ds}{dS}, \quad \lambda_\phi = \frac{r}{R}. \tag{2.2}$$

The capsule membrane is assumed to be the infinitely thin limit of a (3D) incompressible neo-Hookean material. Correspondingly, the principal elastic tensions per unit length **T** are given by[2]

$$T_s = \frac{1}{3\lambda_s\lambda_\phi}\left(\lambda_s^2 - \frac{1}{\lambda_s^2\lambda_\phi^2}\right), \tag{2.3a}$$

$$T_\phi = \frac{1}{3\lambda_s\lambda_\phi}\left(\lambda_\phi^2 - \frac{1}{\lambda_s^2\lambda_\phi^2}\right). \tag{2.3b}$$

Finally, the equilibrium of the shell relates the elastic tensions to the tangential q_s and normal q_n components of the force **q** exerted by the membrane on the fluids,

$$q_s = \frac{dT_s}{ds} + \frac{dr}{rds}(T_s - T_\phi), \tag{2.4a}$$

$$q_n = (K_s T_s + K_\phi T_\phi), \tag{2.4b}$$

where K_s and K_ϕ are the principal curvatures of M.

B. Equations of motion

The motion of the inner and outer fluids obeys the Stokes equations,

$$\nabla.\mathbf{v}=0, \quad \nabla.\boldsymbol{\sigma}=0, \tag{2.5}$$

where $\mathbf{v}$ is the velocity field and where the stress tensor $\boldsymbol{\sigma}$ is given by Newton's law. The associated boundary conditions are:

(i) No flow perturbation far from the particle,
$$\mathbf{v}\to\mathbf{v}^{\infty} \quad \text{as} \quad |\mathbf{x}|\to\infty. \tag{2.6}$$

(i) No-slip and membrane impermeability for $\mathbf{x}\in M$,
$$\mathbf{v}^{\text{int}}(\mathbf{x})=\mathbf{v}^{\text{ext}}(\mathbf{x}) \tag{2.7a}$$
$$=\mathbf{v}^{\mathbf{M}}(\mathbf{x}), \tag{2.7b}$$
$$\mathbf{v}^{\mathbf{M}}(\mathbf{x})=\partial\mathbf{x}(S,t)/\partial t, \tag{2.7c}$$
where $\mathbf{v}^{\text{int}}(\mathbf{x})$ and $\mathbf{v}^{\text{ext}}(\mathbf{x})$ are the velocities in the internal and external fluid. The velocity $\mathbf{v}^{\mathbf{M}}(\mathbf{x})$ of the membrane points is simply the time derivative of their position $\mathbf{x}$, expressed in terms of the Lagrangian variable S.

(ii) Dynamic equilibrium of the membrane,
$$\alpha[\boldsymbol{\sigma}^{\text{ext}}-\boldsymbol{\sigma}^{\text{int}}].\mathbf{n}=-\lambda\mathbf{q}, \tag{2.8}$$
where $[\boldsymbol{\sigma}^{\text{ext}}-\boldsymbol{\sigma}^{\text{int}}]$ denotes the jump in fluid stresses across the membrane, $\mathbf{n}$ is the unit normal vector pointing toward the external fluid, and $\mathbf{q}$ is given by (2.4a) and (2.4b). Parameter α is the time scale ratio $\alpha=t_c/t_0$. However, from (2.8), it is clear the α may also be viewed as a ratio between viscous and elastic forces.

The integral formulation of the Stokes equations leads to a relationship between the elastic force $\mathbf{q}$ exerted by the membrane on the fluids and the unknown velocity of the capsule interface.[8] This formulation is more efficient than the corresponding differential form (2.5), since only the velocity at the boundaries (here the membrane) is determined instead of the full velocity field in the whole flow domain. The axisymmetric integral formulation of the Stokes equations is given by Pozrikidis,[9] where boundary conditions (2.6), (2.7a), (2.7b), and (2.8) are already included,

$$v^{M}{}_{p}(\mathbf{x})-\frac{(1-\lambda)}{8\pi}\int_{C}\underbrace{\{D_{px}(\mathbf{x}-\mathbf{y})[v^{M}{}_{x}(\mathbf{y})-v^{M}{}_{x}(\mathbf{x})]+D_{pr}(\mathbf{x}-\mathbf{y})v^{M}{}_{r}(\mathbf{y})-E_{pr}(\mathbf{x}-\mathbf{y})v^{M}{}_{r}(\mathbf{x})\}ds(\mathbf{y})}_{\text{integral 1}}$$
$$=v^{\infty}{}_{p}(\mathbf{x})-\frac{1}{8\pi}\frac{\lambda}{\alpha}\int_{C}\underbrace{\{J_{px}(\mathbf{x}-\mathbf{y})q_x(\mathbf{y})+J_{pr}(\mathbf{x}-\mathbf{y})q_r(\mathbf{y})\}ds(\mathbf{y})}_{\text{integral 2}} \quad \text{with } p=x,\ r \text{ and } \mathbf{x}\in C, \tag{2.9}$$

where C is a meridian curve of M. The stresslet coefficients (D_{px}, D_{pr}, and E_{pr}) and the Stokeslet coefficients (J_{px},J_{pr}) are given by Pozrikidis.[9] Integral 1 is a regularized form of the double layer integral taken in the principal value sense. Integral 2 is also improper when $\mathbf{y}=\mathbf{x}$, but may be shown to converge since the singularity of the kernel $\mathbf{J}$ is logarithmic.

C. Type of flow

As was mentioned in Sec. I, the primary concern of this study is the investigation of the capsule dynamic behavior. Different types of transient motions are thus considered. In the following, t^* denotes the dimensional time and t the dimensionless time defined as $t=t^*/t_0$.

1. Sudden start of flow

The capsule is at rest and not deformed. At time $t=0$, it is subjected to a pure straining motion of constant intensity $G=G_0$. The obvious time scale is then $t_0=G_0^{-1}$. As a result, the flow field at infinity becomes in dimensionless form,

$$v_x^{\infty}=x, \quad v_r^{\infty}=-\tfrac{1}{2}r, \quad v_{\phi}^{\infty}=0, \tag{2.10}$$

and α may be expressed in terms of the capillary number ε,

$$\alpha=\lambda\varepsilon=\lambda\mu G_0 L/E_s.$$

2. Relaxation after flow cessation

The capsule is first deformed by application of the above procedure. At time $t=0$, the capsule has a given deformation D_0, the flow is stopped ($G=0$), and the capsule is allowed to relax back to its reference shape. The time scale is then $t_0=t_c$, thus $\alpha=1$, $\varepsilon=0$, and $\mathbf{v}^{\infty}=0$.

3. Flow oscillations

The shear rate is assumed to increase and decrease linearly with time, between the values 0 and $G_{\max}$ (this protocol is commonly used in shear viscometers). Correspondingly, the first cycle of oscillation is described by

$$G(t^*)=G_{\max}t^*/T_o, \quad t^*\in[0,T_o],$$
$$G(t^*)=G_{\max}(2-t^*/T_o), \quad t^*\in[T_o,2T_o], \tag{2.11}$$

where $2T_o$ is the dimensional oscillation period. This cycle may be repeated indefinitely. The time scale is set to $t_0=t_c$, and thus $\alpha=1$. A measure of the variable flow strength is given by the maximum capillary number $\varepsilon_{\max}$

$=\mu G_{\max} L/E_s$. An additional parameter enters the problem, namely the time ratio $T=T_o/t_c$. In nondimensional form, the flow field at infinity then becomes

$$v_x^\infty=(\lambda\varepsilon_{\max}t/T)x, \quad t\in[0,T],$$
$$v_x^\infty=[\lambda\varepsilon_{\max}(2-t/T)]x, \quad t\in[T,2T], \tag{2.12}$$

with similar expressions for v_r^∞.

III. NUMERICAL PROCEDURE

The numerical algorithm is presented for case (1) and can be easily extended to the other cases. At time $t=0$, the capsule is in its rest shape and the position of the membrane material points is recorded. The dynamic process is initiated by suddenly applying the straining flow. At any given time step, the calculation involves three phases. First, given the present position of the membrane material points, the metric properties $(\mathbf{n},s,K_s,K_\phi)$, local deformations (λ_s,λ_ϕ), elastic tensions (T_s,T_ϕ), and load (q_s,q_n) on the membrane are computed using (2.2) to (2.4). Next, Eq. (2.9) is solved for the membrane velocity $\mathbf{v}^M$. Finally, the position of the membrane points is updated by means of the kinematic condition (2.7c). This iterative process is stopped when a steady state is reached, that is when the time derivative of the capsule deformation is less than some small preset value (usually 10^{-4}). Further details on the procedure used for the identification of the steady state of the system are given in the next section.

Spatial discretization follows the boundary element method (BEM). The arc length S in the reference state is used as the independent space variable. The capsule meridian C is first partitioned into N two-node elements. The $N+1$ nodal points are unevenly spaced along S with a higher density in areas of large curvature. Cubic B-splines are used as basis functions to interpolate the position of the interface $\mathbf{x}=[x(S,t),r(S,t)]$ as well as the velocity $\mathbf{v}^M$,[10]

$$\begin{bmatrix} x(S,t) \\ r(S,t) \end{bmatrix} = \sum_{j=0}^{N+2} \begin{bmatrix} \xi_j(t) \\ \rho_j(t) \end{bmatrix} BS_j(S), \tag{3.1}$$

$$\begin{bmatrix} v_x^M(S,t) \\ v_r^M(S,t) \end{bmatrix} = \sum_{j=0}^{N+2} \begin{bmatrix} \overline{\omega}_{xj}(t) \\ \overline{\omega}_{rj}(t) \end{bmatrix} BS_j(S), \tag{3.2}$$

where BS_j is a cubic B-spline centered on the jth node, and where $\xi_j,\rho_j,\overline{\omega}_{xj},\overline{\omega}_{rj}$, are the interpolation coefficients. The coefficients corresponding to $j=0$ and $j=N+2$ are computed in terms of the coefficients $\xi_j,\rho_j,\overline{\omega}_{xj}\overline{\omega}_{rj}$, $(j=1...N+1)$, by means of the following relations at the poles of the capsule:

$$\frac{\partial x}{\partial S}=0, \quad \frac{\partial^2 r}{\partial S^2}=0, \quad \frac{\partial v_x}{\partial S}=0, \quad \frac{\partial^2 v_r}{\partial S^2}=0,$$

that follow directly from the axisymmetry of the problem.

Each basis function BS_j is nonzero over only four consecutive elements, namely in the interval $[S_{j-2};S_{j+2}]$, where S_j is the arc length at the jth point. Over each of these four elements, BS_j is a third-order polynomial. It is determined by requiring continuity of the polynomial and of the first and second derivatives at the boundaries of the element.[11] Cubic B-splines are respectively $O(\Delta S^4)$, $O(\Delta S^3)$, and $O(\Delta S^2)$ accurate in interpolating a smooth function, its first and second derivatives (where ΔS denotes a typical element length). The widely used Lagrange basis functions are $O(\Delta S^3)$ and $O(\Delta S^2)$ in interpolating a smooth function and its first derivative, but are unable to interpolate the second derivative. This is in fact the major advantage of B-splines over quadratic Lagrange basis functions. Continuity of the second derivative at the nodes of the interpolant is essential for applications to membrane mechanics problems, since second-order surface properties (curvature) are needed. More details on the application of B-splines in the boundary element method can be found in Pelekasis *et al.*[12]

Then, the B-spline interpolations (3.1) and (3.2) are used in Eq. (2.9). The integrals over C are decomposed into a sum of elementary integrals taken over one boundary element. As explained in Sec. II, integral 1 has been regularized and is therefore integrable via regular quadrature (e.g., five-point Gauss method). Integral 2 is regular except over elements containing point $\mathbf{x}$, where it is logarithmically singular. Over these elements, integration is performed through a 12-point logarithmic quadrature. This ensures that the numerical error is due to the interpolation procedure rather than numerical integration.[13] Requiring Eq. (2.9) to be satisfied at each node leads to a matrix equation

$$\mathbf{L}\begin{bmatrix} \overline{\omega}_x \\ \overline{\omega}_r \end{bmatrix} = \mathbf{H}. \tag{3.3}$$

Matrix $\mathbf{L}$ [dimensions $(2N+2)\times(2N+2)$] contains the stresslet coefficients D_{px},D_{pr},E_{pr}, and vector $\mathbf{H}$ (dimensions $2N+2$) contains the contributions from the far field velocity $\mathbf{v}^\infty$ and from integral 1. The latter can be evaluated at each time step since the load components q_x and q_r are known. The good conditioning of the matrix $\mathbf{L}$ to be inverted is guaranteed by the fact that the integral equation is of the second kind.[14] Equation (3.3) is solved by Gauss elimination.

After the membrane velocity is computed, the position of the membrane points is updated by integrating the kinematic condition (2.7c) by means of a fourth-order explicit Runge–Kutta (RK) scheme. Numerical stability is ensured when the time step Δt is lower than $K(\Delta S)^2$, where K is a coefficient that depends on λ and ε.

Spatial accuracy of the numerical method was verified by means of mesh refinement using a time step $\Delta t=0.005$, low enough to ensure stability for all considered meshes. Increasing the number of nodes from 31 to 61 and from 61 to 121 shows that the numerical error is $O(\Delta S^2)$. For example, for a spherical capsule and $\varepsilon=0.05$, the computed steady deformed shapes are identical up to the third significant digit for 61 and 121 points. Despite the more complicated form of the kernels and the different flow regimes encountered here, the present scheme exhibits the same stability and accuracy characteristics as the one presented by Pelekasis *et al.*[12] In their algorithm, a fourth-order RK scheme is also employed, in conjunction with the boundary element method with B-splines forming the set of basis functions, for the solution of free surface problems in the potential flow regime. This is an indication of the range of validity and robustness of the boundary integral formulation.

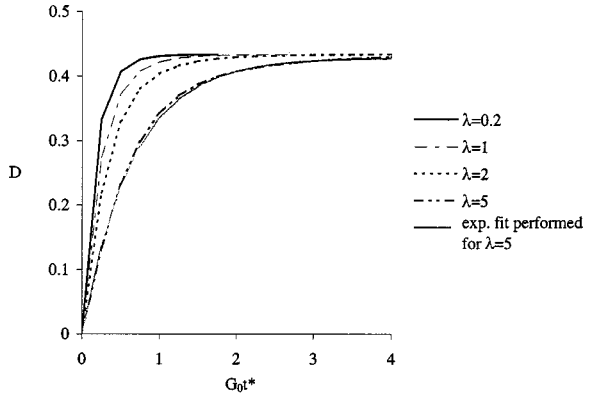

FIG. 2. Evolution of the deformation versus time of an initially spherical capsule for different viscosity ratios $\lambda(\varepsilon=0.05)$. For $\lambda=5$, comparison between exponential fit and numerical results.

As the capillary number ε increases, the magnitude of deformation increases as well, but the accuracy in the converged shapes does not exhibit any significant deterioration until ε approaches the critical value ε_c beyond which no steady state exists. It should also be noted that for 61 points, a typical case ($\varepsilon=0.05,\lambda=2,A=B=1$) takes 30 min CPU to run on a PC Dell pro200.

IV. RESULTS

A. Definition of deformation

The deformation of an axisymmetric capsule is measured by parameter $D(t)$,

$$D(t)=\frac{a(t)/A-b(t)/B}{a(t)/A+b(t)/B}, \quad D\in[0;1], \tag{4.1}$$

where $a(t)$ and $b(t)$ are, respectively, the capsule half diameter and radius at time t. This definition reduces to the classical Taylor deformation for droplets when the capsule is initially spherical.

The time evolution of $D(t)$ is obtained numerically, but it turns out that in case (1) an exponential fit may be performed on all the numerical results with a correlation coefficient R^2 larger than 0.98 (Fig. 2),

$$D(t^*)=D_\infty(1-e^{-t^*/\tau_s}). \tag{4.2}$$

Consequently, the dynamic response of the capsule may be characterized with only two parameters: the deformation at steady state D_∞ and the dimensional response time τ_s. Similarly, for capsule relaxation (case 2), an exponential fit of the numerical results can also be performed,

$$D(t^*)=D_0e^{-t^*/\tau_r}, \tag{4.3}$$

where τ_r is a dimensional relaxation time ($R^2>0.98$). The results presented here have been obtained for the case where D_0 is the steady deformation corresponding to a constant capillary number ε_0.

The analytical model of Barthès-Biesel and Rallison, which is restricted to initially spherical capsules subjected to small deformations, also finds that the deformation is an exponential function of time. However, for a capsule with a Mooney–Rivlin membrane, there are two characteristic response times. The ratio between those two times is roughly 10 for $\lambda=0$ and 5 for $\lambda=5$. Consequently, except during the initial instants, the time response of the capsule is essentially governed by the smallest of the two characteristic times. The analytical values for the steady deformation $D_{\infty a}$ and for the dimensionless characteristic time $G_0\tau_a$ needed for the capsule to reach steady state are then given by

$$D_{\infty a}=75\varepsilon/4, \tag{4.4a}$$

$$G_0\tau_a=\varepsilon\frac{3(19\lambda+16)(2\lambda+3)}{5(19\lambda+24)-\sqrt{5277\lambda^2+14\,256\lambda+9792}}, \quad \varepsilon\ll 1. \tag{4.4b}$$

TABLE I. Comparison between numerical and analytical solutions for the final deformation and response time for a spherical capsule and $\epsilon=10^{-3}$.

λ	$G_0\tau_s$	$G_0\tau_a$	D_∞	$D_{\infty a}$
0.2	0.0076	0.0078	0.0181	0.018 75
1	0.0115	0.0120	,,	,,
5	0.0310	0.0331	,,	,,

It is, however, quite surprising to find that this simple exponential time dependence persists even when the problem is fully nonlinear, i.e., when the membrane, which is a free surface characterized by a nonlinear behavior, is subjected to large deformations. This might be due to the fact that the external flow is linear. However, in spite of the simple time dependence, *the evolution of deformation cannot be determined without a numerical computation.* The parameter D_∞ remains an unknown complicated function of capillary number and initial shape. The same holds for τ_r and τ_s which depend, in addition, on the viscosity ratio.

The steady state has already been studied by Li *et al.* for capsules with different membrane constitutive laws and initial shapes. In particular, they find that there is a critical value ε_c of the capillary number past which no steady state exists. Therefore, in this work we will focus on the transient phase of the capsule deformation.

B. Validation of results

The capsule deformation is computed in case (1), for a spherical capsule ($A=B=1$) and for different values of ε and λ, with ε remaining below the critical value $\varepsilon_c\sim 0.08$. The elongational flow has constant intensity G_0. Throughout this series of tests 61 nodal points are used along the capsule meridian with a time step adapted to the values λ and ε. A global estimate of the precision of the numerical method is given by the final volume variation between the initial and steady deformed shapes, which should be zero in principle. In all cases, the volume variation was less than 0.04% of the capsule initial volume.

The numerical results are also compared against the analytical predictions (4.4a) and (4.4b). For $\varepsilon=10^{-3}$, the numerical results are in good agreement with the analytical predictions (Table I). At steady state, the symmetry of the problem implies that the internal liquid is at rest. Conse-

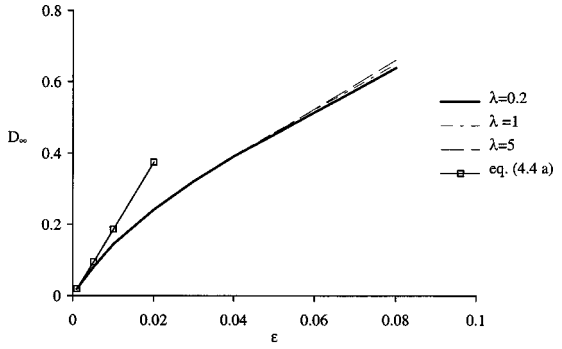

FIG. 3. Steady-state deformation versus ε for an initially spherical capsule and for different viscosity ratio λ.

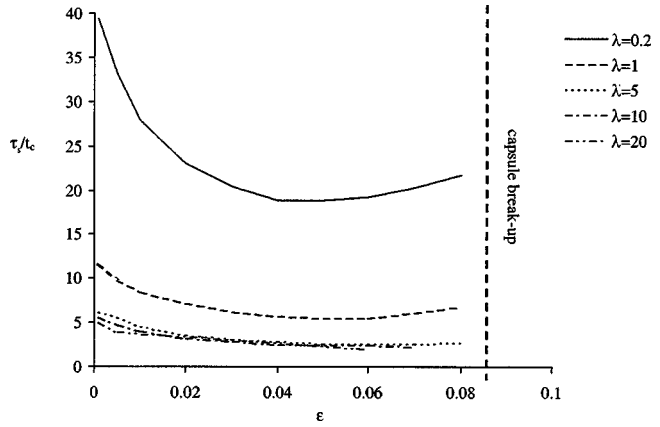

FIG. 5. Intrinsic response time versus capillary number ε for an initially spherical and for different viscosity ratios λ.

quently, the steady deformation should not depend on λ, which is indeed the case as can be seen from Table I, at least within the accuracy of the numerical calculation and of the exponential fit.

The time evolution of the deformation of a spherical capsule is shown in Fig. 2 for $\varepsilon=0.05$. It is clear that the deformation converges to the same steady value for different viscosity ratios. As ε increases, it is also found that the steady deformation does not depend on λ (Fig. 3). It also agrees with the results previously obtained by Li *et al.* for spherical capsules with $\lambda=1$. Figure 3 also shows that, for small deformations, the numerical and asymptotic results are in good agreement within about 15% up to $\varepsilon=0.005$. In agreement with Li *et al.*, a critical value ε_c of the capillary number ($\varepsilon_c \in]0.08;0.09]$) is also found past which no steady state exists. Then for $\varepsilon>\varepsilon_c$, the capsule continuously extends until burst occurs. Also apparent in Fig. 3 is a noticeable trend of the curves to deviate from each other as ε approaches ε_c. This is not due to numerical error, but might be a consequence of the exponential fit that is used to determine D_∞. As $\varepsilon \to \varepsilon_c$, a steady state no longer exists and an exponential fit may no longer be appropriate.

C. Transient response

1. Response to a sudden start of flow

An initially spherical unstressed capsule is subjected to a sudden start of a flow with constant capillary number ε and intensity G_0. Figure 4 shows the variation of the dimensionless response time $G_0\tau_s$ versus ε for different values of λ. The capsule response time is a nonlinear function of ε. It increases sharply with λ and ε, and consequently with increasing viscosity of the internal and external fluids. This behavior is due to the complex interaction between the hydrodynamic stresses that deform the membrane and the elastic tensions that resist the deformation. Furthermore, Fig. 4 shows that small deformation theory overestimates the values of the response time. The range of validity of the analytical solution for τ is found to be the same as for the deformation. Figure 5 shows the ''intrinsic'' response time τ_s/t_c as a function of ε for the same range of values of λ. When $\lambda<5$ and when ε is small, τ_s/t_c decreases sharply as ε increases. More specifically, when ε increases from 0.001 to 0.05, the relative decrease of τ_s/t_c is roughly 60%. For a given capsule, this indicates a significant reduction in the dimensional response time τ_s with increasing flow strength. As ε further increases from 0.05 to 0.08, the maximum relative variation of τ_s/t_c is 15%. When λ is larger than 5, it has no influence on τ_s/t_c and τ_s is thus proportional to the viscosity of the internal fluid.

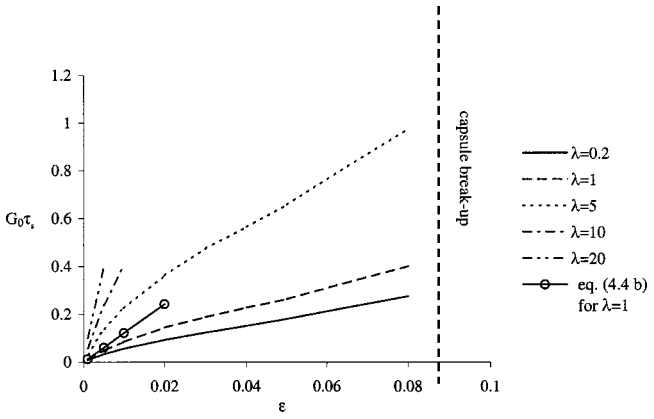

FIG. 4. Dimensionless response time versus capillary number ε for an initially spherical capsule and for different viscosity ratios λ.

Figure 5 indicates that the capsule response time is determined by the larger of two time scales, namely G_0^{-1} and t_c. When G_0 is small, G_0^{-1} is large and determines the capsule response: hence the significant influence of ε on the response time for $\varepsilon<0.05$. As G_0 (and ε) increases, the relative magnitude of the intrinsic time scale increases, $t_c/G_0^{-1}=\lambda\varepsilon$, until it dominates the dynamics of the flow, making τ_s almost independent on the characteristics of the external flow.

The effect of capsule initial geometry is assessed by comparing the dynamic behavior of four isovolumic spheroids: oblate ($A/B=0.46,0.75$), prolate ($A/B=1.33$), and spherical ($A=B=1$). For given values of ε and for moderately large values of $\lambda(\lambda<5)$, the intrinsic response time τ_s/t_c decreases as A/B increases (Tables II and III). This is due to the fact that an initially prolate profile is closer to the corresponding equilibrium profile (elongated along the x axis) than oblate or spherical shapes. A comparison between the initial and deformed profiles at equilibrium is shown on

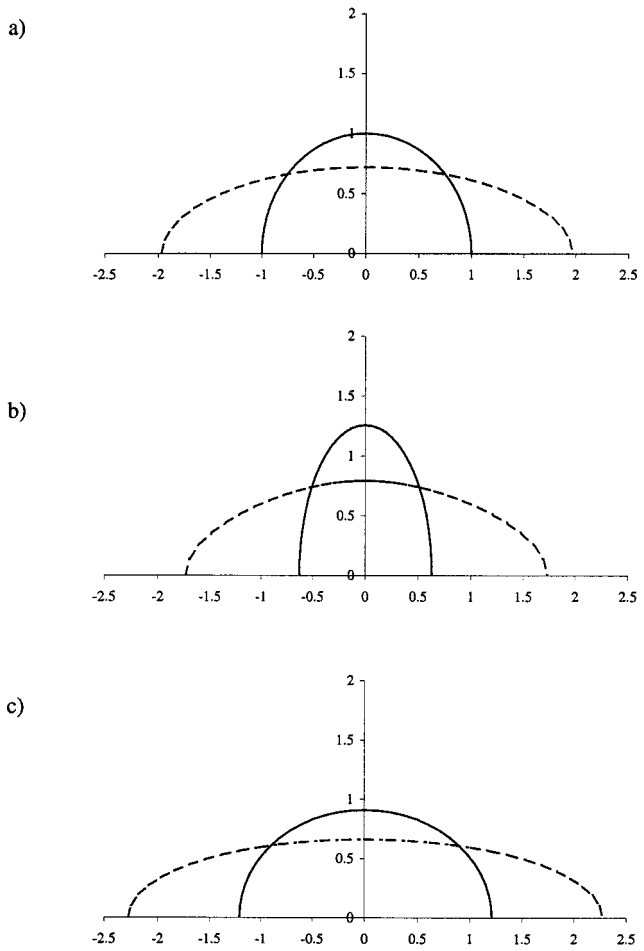

FIG. 6. Initial capsule profile and steady deformed profile for $\varepsilon=0.05$ and (a) $A/B=1$, (b) $A/B=0.5$, and (c) $A/B=1.33$ (solid line: initial profile, dashed line: steady profile).

Fig. 6 for $\varepsilon=0.05$, $\lambda=1.0$, and $A/B=0.75$, 1.0, 1.33, respectively. It should also be noted that the effect of initial shape on the response time is more important for small capillary numbers ($\varepsilon=0.01$) than for larger values ($\varepsilon=0.05$). The same trend is also observed for the steady deformation D_∞ (Tables II and III). This indicates a partial loss of memory, as far as the capsule initial configuration is concerned, when the relative importance of the viscous stresses is increased.

2. Capsule relaxation

The relaxation time τ_r/t_c and the response time τ_s/t_c are compared on Fig. 7 for $\lambda=1$ and for an initially spherical capsule. For small deformations, $\varepsilon<0.005$, the two times are roughly equal to the value predicted by the small perturbation theory. For larger deformations the relaxation time τ_r is significantly larger than τ_s. Figure 7 clearly illustrates the fact that capsule deformation following a sudden start of flow and capsule relaxation are two different processes. Indeed, during relaxation, it is only the energy stored in the membrane that is used to move both the internal and external liquids. In the case of a sudden start of flow, energy is continuously provided to the system (capsule plus suspending fluid), resulting in the motion of the two liquids and membrane deformation. A similar difference between τ_r and τ_s is also observed for other values of λ.

TABLE II. Dimensionless response time and steady deformation for four isovolumic capsules with different aspect ratios and for $\epsilon=0.01$.

	$A/B=0.46$	$A/B=0.75$	$A/B=1$	$A/B=1.33$
$\tau_s/t_c(\lambda=0.2)$	45.9	38.2	28.0	22.5
$\tau_s/t_c(\lambda=1)$	14.2	11.4	8.47	6.54
$\tau_s/t_c(\lambda=5)$	8	6.46	4.50	3.32
D_∞	0.31	0.19	0.14	0.10

TABLE III. Dimensionless response time and steady deformation for four isovolumic capsules with different aspect ratios and for $\epsilon=0.05$.

	$A/B=0.46$	$A/B=0.75$	$A/B=1$	$A/B=1.33$
$\tau_s/t_c(\lambda=0.2)$	23.6	18.4	18.0	17.8
$\tau_s/t_c(\lambda=1)$	7.01	5.53	5.26	5.51
$\tau_s/t_c(\lambda=5)$	3.92	2.93	2.63	2.47
D_∞	0.64	0.51	0.46	0.43

3. Periodic variation of strain

An initially spherical capsule is now placed in the transient flow given by (2.11). The capillary number oscillates between 0 and $\varepsilon_{\max}$, with period $2T_o$ (Fig. 8). A dimensional analysis of the problem shows that there are now four relevant time scales, namely t_c, $G_{\max}^{-1}$, the momentum diffusion time scale L^2/ν (ν denotes the kinematic viscosity of the external fluid), and the oscillation period $2T_o$. A measure of the relative importance of momentum diffusion in the two liquids and momentum imparted to the system due to the oscillatory variation of the rate of strain is the Womersley number,

$$Wo=L/(\nu T_o)^{1/2}.$$

Here, it is assumed that $Wo\ll 1$, so that transient inertia effects are also neglected. Consequently, the problem is still quasisteady.

The history of capsule deformation is shown on Fig. 8 for $A/B=1$, $T_o/t_c=5.26$, $\lambda=1$. After a transient phase, the capsule reaches a dynamic equilibrium where the global deformation $D(t)$ oscillates about a mean value, D_{mean}. The internal fluid viscosity causes a time delay δ, between the variations of capillary number and of deformation. Corre-

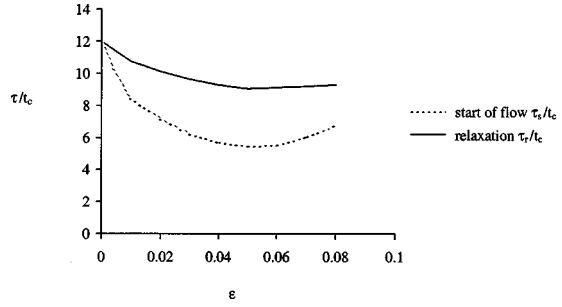

FIG. 7. Intrinsic response and relaxation time for an initially spherical capsule and for $\lambda=1$.

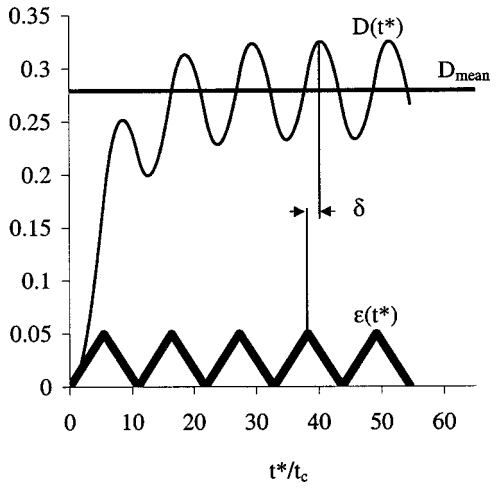

FIG. 8. Deformation and capillary number versus time for $\varepsilon_{\max}=0.05$, $\lambda=1$ and $T_o=5.26t_c$ and $A/B=1$.

spondingly, the dynamic response of the capsule may be characterized by the following parameters: the number of cycles N_c needed to reach dynamic equilibrium, the mean deformation D_{mean}, the oscillation amplitude, and the phase shift δ/T_o.

As an example, let us consider a spherical capsule with viscosity ratio $\lambda=1$ and subjected to oscillations with $\varepsilon_{\max}=0.05$ (Table IV). It should be noted that the Womersley number can be expressed as a function of the particle Reynolds number $\text{Re}=G_{\max}L^2/\nu$ and the problem parameters,

$$W_o=\text{Re}\frac{1}{\lambda\varepsilon}\frac{t_c}{T_0}.$$

For a given value of T_0/t_c and for a given capsule, the hypothesis $Wo\ll 1$ remains valid for any values of Re and $\varepsilon_{\max}$ such that: $\text{Re}/\varepsilon_{\max}\ll T_o/t_c\lambda$.

In the case where $T_o/t_c\gg 1$ (e.g., $T_o/t_c=100$), the time variations are slow enough for the capsule to adapt and to be always in dynamic equilibrium with the external flow [Fig. 9(a)]. Over one period, the capsule deformation varied between 0.05 and a maximum value equal to $D_\infty(\varepsilon_{\max})$ within 2%. Consequently D_{mean} is equal to $1/2D_\infty(\varepsilon_{\max})$ within 9%.

For intermediate values of the oscillation frequency (e.g., $T_o/t_c=5.26$), it takes a finite number of cycles to reach dynamic equilibrium ($N_c\cong 4$). The mean deformation is almost equal to $D_\infty(1/2\varepsilon_{\max})$ and the oscillation amplitude is of the order of 14% of D_{mean} [Fig. 9(a)].

When $T_o/t_c\ll 1$ (e.g., $T_o/t_c=0.5$), the time variations of ε are too fast for the capsule to follow them, and it thus takes a large number of cycles ($N_c=60$) to reach dynamic equilibrium [Fig. 9(b)]. The capsule barely deforms between two consecutive cycles and the dynamic response curve oscillates about the steady deformation corresponding to a sudden start of flow with $1/2\varepsilon_{\max}$. At dynamic equilibrium, the amplitude of the oscillation is 1.5% of D_{mean}. Then $D_{\text{mean}}\cong D_\infty(1/2\varepsilon_{\max})$ and the time τ_d necessary to reach this dynamic equilibrium is about equal to $\tau_s(1/2\varepsilon_{\max})$.

Furthermore, a capsule can sustain, without breaking, shear rates greater than the stationary critical shear rate $\varepsilon_c(\varepsilon_c\in]0.08;0.09])$ provided that T_0/t_c is small. Figure 10(a) shows deformation versus time for $T_0/t_c=0.1$, $\varepsilon_{\max}=0.14$, 0.16, 0.19. The first two values of $\varepsilon_{\max}$ are such that $\varepsilon_{\max}<2\varepsilon_c$. Then the capsule reaches a dynamic steady state and oscillates around a final steady deformation. The case $\varepsilon_{\max}=0.19$ corresponds to a value larger than $2\varepsilon_c$. The dynamic deformation curve diverges and the capsule will eventually burst. Figure 10(b) shows a comparison of the transient responses to a steady shear rate $\varepsilon=0.08$ and to a dynamic shear rate $\varepsilon_{\max}=0.16$ and $T_0/t_c=0.1$. The dynamic equilibrium deformation is slightly smaller than $D_\infty(1/2\varepsilon_{\max})$ and τ_d is about twice $\tau_s(1/2\varepsilon_{\max})$. It is clear that the maximum transient shear rate that a capsule can sustain without

TABLE IV. Dynamic response of a spherical capsule for period of oscillation of the external flow in the range $[0.1t_c;100t_c]$. Here, $\lambda=1$, $A/B=1$, and $\epsilon_{\max}=0.05$. The value of τ_s corresponds to the one obtained for a sudden start of flow with $\epsilon=\epsilon_{\max}$.

T_o/t_c	T_o/τ_s	D_{mean}	δ/T_o	Oscillation amplitude (% of D_{mean})	N_c
0.1	0.019	0.280	−0.6	0.2	>200
0.5	0.095	0.280	−0.5	1.5	60
2.5	0.475	0.280	−0.45	7.5	8
5	0.95	0.280	−0.4	15	3.5
10	1.9	0.276	−0.35	28	1.5
25	4.75	0.267	−0.16	53	0.5
100	19	0.25	−0.06	80	⋯

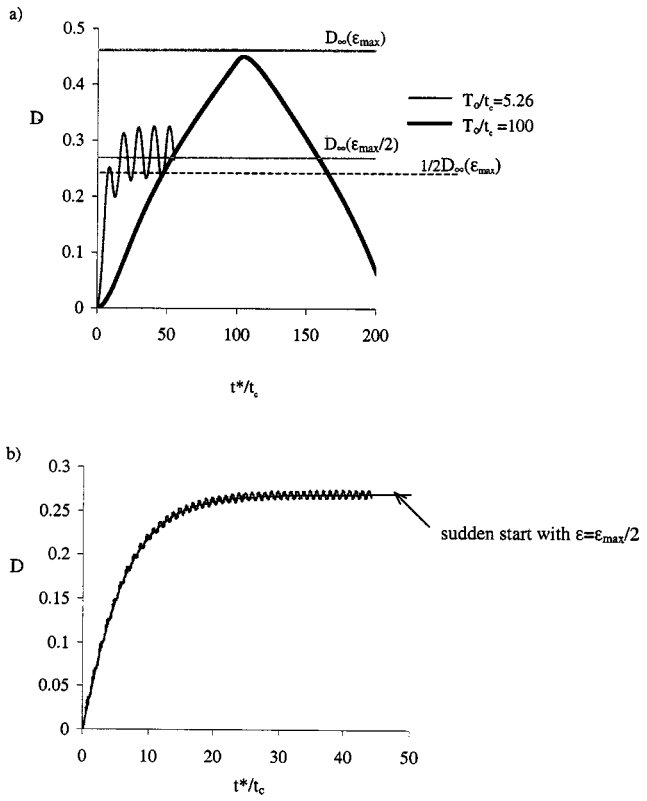

FIG. 9. (a) Global deformation versus time for an initially spherical capsule, for $\lambda=1$ and for different oscillation time T_o. (b) Global deformation versus time for an initially spherical capsule, $\lambda=1$, $\varepsilon_{\max}=0.05$, and $T_o=0.5t_c$.

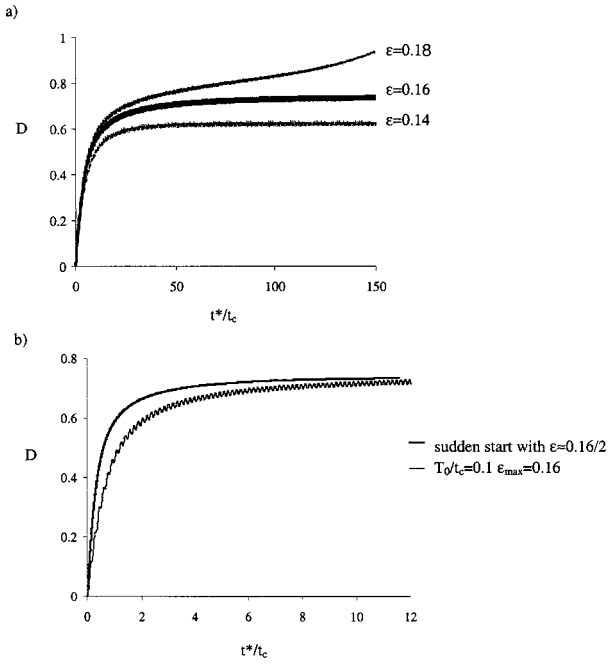

FIG. 10. (a) Global deformation versus time for $\varepsilon_{\max}=0.14$, 0.16, 0.19, and $T_0=0.1t_c$ (initially spherical capsule, $\lambda=1$). (b) Global deformation versus time for $\varepsilon_{\max}=0.16\approx 2\varepsilon_c$ and $T_0=0.1t_c$ compared to global deformation versus time for $\varepsilon=\varepsilon_{\max}/2$ (initially spherical capsule, $\lambda=1$).

breaking depends on the value of T_0/t_c. A detailed study has not been done, so it can only be concluded that the value of $\varepsilon_{\max}$ must be smaller than $2\varepsilon_c$.

Table IV shows that, as T_o/t_c increases from 0.1 to 100, there is a gradual decrease of D_{mean}. This is due to the fact that D_∞ is a nonlinear function of ε (Fig. 3) and thus $1/2D_\infty(\varepsilon_{\max})<D_\infty(1/2\varepsilon_{\max})$. Also, the oscillation amplitude increases and the number of cycles decreases when T_o/t_c increases. Another important aspect concerns the phase shift which measures the delay between the capsule deformation and the externally imposed shear rate. The capsule dynamic response results from two interrelated effects: an elastic response due to the membrane and a viscous response due to the internal fluid. The smaller δ, the larger the relative importance of the elastic response. For a given capsule (with a given t_c), the time delay δ increases when T_o/t_c increases. This is to be expected, since for small values of T_o/t_c, the capsule barely deforms and there is almost no internal fluid motion and thus no viscous effects. For large values of T_o/t_c, there is a significant internal motion, and thus comparatively large viscous effects.

TABLE V. Dynamic response of a spherical capsule for $\varepsilon_{\max}=0.05$. Capsules 1, 2, and 3: $T_o=10\mu A/E_s$. Capsules 4, 5, and 6: $T_o=\tau_s$.

	λ	T_o/t_c	T_{o/τ_s}	D_{mean}	δ/T_o	Oscillation amplitude (% of D_{mean})	N_c
Capsule 1	1	10	1.9	0.276	−0.35	28	1.5
Capsule 2	3.7	2.7	0.95	0.280	−0.4	16	3.5
Capsule 3	8.9	1.12	0.475	0.280	−0.45	8	8
Capsule 4	0.2	18	1	0.279	−0.4	16	2.5
Capsule 5	1	5.26	1	0.278	−0.4	16	2.5
Capsule 6	5	2.63	1	0.278	−0.37	16	2.5

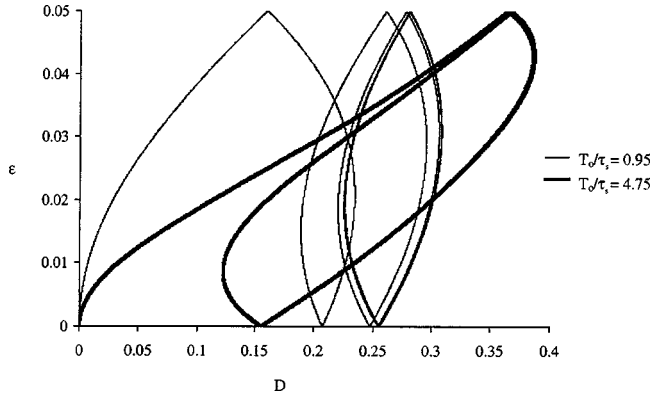

FIG. 11. Capillary number ε versus deformation for a capsule with viscosity ratio $\lambda=1$, for $\varepsilon_{\max}=0.05$, $T_o/\tau_s=0.95$, and $T_o/\tau_s=4.75$ ($A/B=1$).

Table V compares the response of spherical capsules with same radius A, same elastic modulus E_s, but with different values of the internal viscosity $\lambda\mu$. These capsules are placed in the same fluid (viscosity μ) and subjected to the same maximum rate of strain ($\varepsilon_{\max}=0.05$). The response time τ_s of each capsule for a sudden start of flow with intensity $\varepsilon_{\max}$ can thus be determined. As was shown earlier, τ_s depends on λ. For capsules 1, 2, 3 the oscillation period is set to $T_o=10\mu A/E_s$ and thus the ratio T_o/τ_s varies roughly from 0.5 to 2. When T_o/τ_s decreases, the mean deformation does not change much, but the phase shift and N_c increase whereas the oscillation amplitude decreases. The results are identical to those obtained for $\lambda=1$ for the same value of T_o/τ_s (Table IV). For capsules 4, 5, 6, the oscillation period T_o is adapted so that the ratio T_o/τ_s is equal to unity. The dynamic response of these three capsules is then identical. The conclusion is that rather than the ratio T_o/t_c, it is the ratio T_o/τ_s that controls the capsule response. Given the period of the external flow, the phase shift δ increases with increasing capsule viscosity or increasing values of λ (Table V). One can also anticipate that δ will increase with increasing value of $\varepsilon_{\max}$, given the rest of the problem parameters, since this amounts to decreasing capsule elasticity.

It is possible to plot the capsule deformation versus capillary number (Fig. 11). The corresponding graphs are significantly different depending on the value of T_o/τ_s. For large values (e.g., $T_o/\tau_s=4.75$), the equilibrium is reached within one cycle, and the hysteresis area is large. For $T_o/\tau_s=O(1)$, equilibrium is reached after three cycles, and the hysteresis area is smaller than in the previous case.

V. CONCLUSION

The numerical model allows prediction of the transient response of a capsule to a change of flow conditions. This study has focused on the role of geometry and internal viscosity.

It is of interest to compare the present results to some results obtained by Ramanujan and Pozikidis[7] for a capsule suspended in a simple shear flow. To facilitate the compari-

TABLE VI. Comparison between the response times of a capsule subjected to the sudden start of different shear flows. The superscript ss and el refer, respectively, to simple shear flow or to elongational flow. The simple shear results are estimated from the graphs of Ramanujan and Pozrikidis.

D_∞	$G^{ss}\tau^{ss}$	ϵ^{ss}	$G^{el}\tau^{el}$	ϵ^{el}	τ^{el}/τ^{ss}
		$\lambda=1$			
0.16	0.3	0.025	0.084	0.01	0.7
0.26	0.41	0.05	0.14	0.02	0.85
0.38	0.7	0.1	0.23	0.04	0.8
		$\lambda=0.2$			
0.26	0.3	0.05	0.09	0.02	0.75
0.4	0.5	0.1	0.15	0.04	0.75

son, the superscripts el and ss refer, respectively, to the elongational flow (2.1) and to a simple shear flow in the *x*-*y* plane ($v_x=G^{ss}y$, $v_y=v_z=0$). Ramanujan and Pozikidis use essentially the same technique as we do, but their model is three dimensional. The time evolution of deformation is shown after sudden start of flow, for $\lambda=1$ and $\lambda=0.2$ (their Figs. 4 and 5, respectively) and for different values of the capillary number ε^{ss}. It is possible to fit approximately an exponential function to the deformation curves obtained for moderate values of ε^{ss}. This allows the estimation of a response time τ^{ss} (for large values of ε^{ss}, a deformation overshoot is observed and there is no exponential fit). Of course, a simple shear and a pure straining motion correspond to very different flow situations and it is thus difficult to compare the responses of a given capsule when it is subjected to either flow field. For example, identical values of the capillary numbers ε^{ss} and ε^{el} in, respectively, simple shear flow and elongational flow, lead to different values of the capsule deformation. In order to compare the two flow situations, it was decided to consider capsules with the *same steady deformation*. Assuming also that the two particles are identical, the time scale ratio is equal to the capillary number ratio for the two flows,

$$t_0^{el}/t_0^{ss}=G^{ss}/G^{el}=\varepsilon^{ss}/\varepsilon^{el}.$$

The comparison between simple shear and elongational response time is shown in Table VI, where it should be kept in mind that the simple shear values have been estimated from graphical results and are thus not very precise. It is very interesting to note that this ratio remains almost constant and is of order 1. This means that the elongational model might be relevant to estimate the transient response characteristic of a given capsule subjected to more complicated flows at least for small values of the capillary number and the viscosity ratio. The great advantage of the elongational model is that it is axisymmetric and simple to use and that it runs quickly on an average computer. However, for larger values of ε, due to the nonlinear nature of the problem, significant differences in the capsule dynamics might arise between the two different flow configurations. It would be interesting to investigate this point further. Another important result is that, for periodic variations of the rate of strain, the response of the capsule is controlled by the ratio T_o/τ_s. The response time τ_s appears to be the appropriate parameter to estimate the capsule adaptability to changing flow conditions. Finally, this model can obviously be extended to complex membrane constitutive behavior.

ACKNOWLEDGMENTS

The authors wish to thank Professor C. Pozrikidis for providing the full expressions of the boundary integral kernels. This work was supported in part by the bilateral Franco-Hellenic research program PLATO. N.P. would also like to acknowledge support by GSRT under the PENED 95 Grant No. 27.

[1] D. Barthès-Biesel and J. M. Rallison, ''The time independent deformation of a capsule freely suspended in a linear flow,'' J. Fluid Mech. **113**, 251 (1981).
[2] X. Z. Li, D. Barthès-Biesel, and A. Helmy, ''Large deformations and burst of a capsule freely suspended in an elongational flow,'' J. Fluid Mech. **187**, 179 (1988).
[3] C. Pozrikidis, ''The axisymmetric deformation of a red blood cell in uniaxial straining Stokes flow,'' J. Fluid Mech. **216**, 231 (1990).
[4] C. Quéguiner and D. Barthès-Biesel, ''Axisymmetric motion of capsules through cylindrical channels,'' J. Fluid Mech. **348**, 349 (1997).
[5] H. Zhou and C. Pozrikidis, ''Deformation of liquid capsules with incompressible interfaces in simple shear flow,'' J. Fluid Mech. **283**, 175 (1995).
[6] C. Pozrikidis, ''Finite deformation of liquid capsules enclosed by elastic membranes in simple shear flow,'' J. Fluid Mech. **297**, 123 (1995).
[7] S. Ramanujan and C. Pozrikidis, ''Deformation of liquid capsules enclosed by elastic membrane in simple shear flow: Large deformation and effect of fluids viscosities,'' J. Fluid Mech. **361**, 117 (1998).
[8] J. M. Rallison and A. Acrivos, ''A numerical study of the deformation and burst of a viscous drop in an extensional flow,'' J. Fluid Mech. **89**, 191 (1978).
[9] C. Pozrikidis, ''The instability of a moving viscous drop,'' J. Fluid Mech. **210**, 1 (1990).
[10] N. A. Pelekasis, J. A. Tsamopoulos, and G. D. Manolis, ''Equilibrium shapes and stability of charged and conducting drops,'' Phys. Fluids A **2**, 1328 (1990).
[11] C. Deboor, *A Practical Guide to Splines* (Springer, New York, 1978).
[12] N. A. Pelekasis, J. A. Tsamopoulos, and G. D. Manolis, ''A hybrid finite-boundary element method for inviscid flows with free surface,'' J. Comput. Phys. **101**, 231 (1992).
[13] A. H. Stroud and D. Secrest, *Gaussian Quadrature Formulas* (Prentice-Hall, Englewood Cliffs, NJ, 1966).
[14] S. Kim and S. J. Karrila, *Microhydrodynamic*: Principles and selected applications (Butterworth-Heinemann, Washington, D.C., 1991).